INFRARED AND MID-VISIBLE OPTICAL PROPERTIES OF TITAN HAZE AEROSOL ANALOGS.
C. A. Hasenkopf[1,2], C. J. Long[3], R. K. Lessard[2,3], M. R. Beaver[4], M. G. Trainer[5], H. L. Dewitt[2,3], M. A. Freedman[2], O. B. Toon,[1,6], C. P. McKay[7], and M. A. Tolbert [2,3], [1]Department of Atmospheric and Oceanic Sciences, University of Colorado, Boulder, CO 80309, [2]Cooperative Institute for Research in the Environmental Sciences, CIRES, University of Colorado, Boulder, CO 80309, [3]Department of Chemistry, University of Colorado, Boulder, CO 80309, [4]Division of Geological and Planetary Sciences, California Institute of Technology, Pasadena, CA 91125, [5]NASA Goddard Space Flight Center, Greenbelt, MD 20771, [6]Laboratory for Atmospheric and Space Physics, University of Colorado, Boulder, CO 80309, [7]Space Science Division, NASA Ames Research Center, Moffett Field, CA 94503

Introduction: Optical properties of laboratory analogs of Titan aerosol provide insight into the chemical and physical nature of aerosol in the actual Titan atmosphere. Additionally, optical properties dictate the aerosol's important role in the radiative balance of Titan's atmosphere, and, accordingly, Titan's climate. Studying how these optical properties change as a function of CH_4 content in analog gas mixtures used to generate these aerosols may be key to understanding past and future effects of the aerosol on the atmosphere's radiative balance and climate. We report optical properties of Titan analog aerosol in the mid-visible and infrared (IR).

In the visible, the real and imaginary refractive indices at λ = 532 nm were determined using a flow system and cavity ringdown aerosol extinction spectroscopy (CRD-AES). This method, though limited to discrete wavelengths, is unique in that it analyzes aerosol as freely-floating particles instead of collected films.

For the IR studies, aerosol generated from mixtures of varying amounts of CH_4 in N_2 were deposited on films and analyzed with a Fourier Transform IR spectrometer (FT-IR), which generates a continuous transmission spectrum from 2.5 μm – 10 μm. Our results are compared with optical properties from other laboratory analogs and with recent observations from the Visual and IR Mapping Spectrometer (VIMS).

Experimental Method: Figure 1 shows the experimental schematic for the CRD-AES system.

Aerosol generation for CRD-AES system. A gas mixture of 0.1% CH_4 in N_2 is allowed to diffusively mix. This gas mixture is selected because it provides the most instrumental signal. The gases are then flowed into a reaction chamber, where they are exposed to a deuterium lamp that emits continuum radiation from λ = 115 – 400 nm, peaking at 160 nm. Aerosol are generated at a temperature of 20 °C and a pressure of 600 Torr. Aerosol generated from a 0.1% CH_4 with a continuum UV lamp have been found to have a similar chemical composition to those generated at a more Titan-like 2% CH_4 concentration [1].

CRD-AES Measurements and Analysis. The aerosol are then directed into a differential mobility analyzer (DMA), where they are size-selected before entering

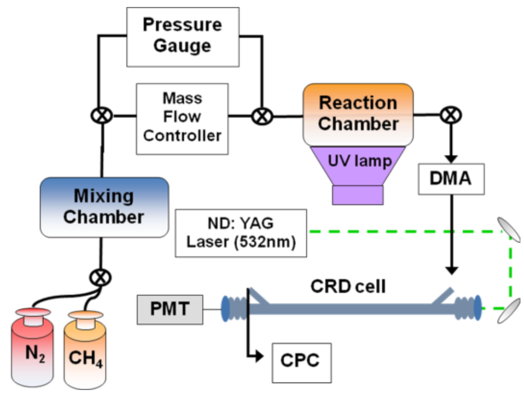

Figure 1: CRD-AES system.

the CRD-AES. The extinction of the aerosol is measured in the CRD-AES, and the exiting particles enter a condensation particle counter (CPC), in which the concentration of the particles is measured. In this manner, the aerosol are analyzed *in situ*, without the need for impaction, minutes after their creation. Applying Mie theory to the extinction and concentration measurements of singly-sized aerosol over a range of sizes allows the real and imaginary refractive indices to be calculated. We model the measured extinction as:

$$b_{ext} = Q_{ext}(n,k,D,\lambda)D^2\left(\frac{\pi N}{4}\right)$$

where b_{ext} is the extinction (cm^{-1}) and N is the particle concentration by volume (particles cm^{-3}). The extinction efficiency Q_{ext} is a function of the particle's diameter D and real (n) and imaginary (k) refractive indices. We vary n and k over a physically reasonable range. The pair of values that yield the minimum reduced Cumulative Fractional Difference (CFD_R) are the best-fitting:

$$\boldsymbol{CFD_R} = \frac{1}{\boldsymbol{P}}\sum_{\boldsymbol{All\ Sizes}} \frac{\left|\boldsymbol{b_{ext-measured}} - \boldsymbol{b_{ext-Mie}}\right|}{\boldsymbol{b_{ext-measured}}}$$

Aerosol generation, collection, and analysis for FT-IR studies. Figure 2 shows the collection schematic for the FT-IR studies. Aerosol analogs are generated in a similar manner to the ones used in the CRD-AES system; however, a different energy source is used for the FT-IR studies and different mixtures of CH_4 in N_2. An electrical discharge source (Tesla coil) is used

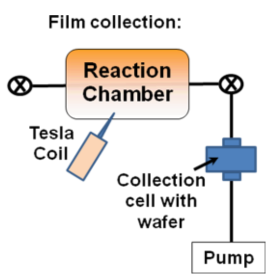

Figure 2: Aerosol generation and collection schematic for FT-IR studies.

instead of the continuum UV lamp. This energy source represents the energetic electrons that bombard the top of Titan's atmosphere. Also, an electrical discharge source produces more material over a shorter span of time than the UV source and is therefore more efficient for collection studies. Once generated, the particles are impacted onto an NaCl substrate, which is held inside an inline filter holder. Depending on the gas mixture used, the collection continues for hours to days.

Results: From the CRD-AES studies, we measure a real refractive index of n = 1.35±0.01 and an imaginary refractive index k = 0.023±0.007 at λ = 532 nm. Figure 3 shows a comparison of these values with other studies. All studies differ in their use of energy source, atmospheric mixture, and/or reaction pressure. Our Titan aerosol analog refractive index has the smallest real refractive index reported, and an imaginary refractive index that is comparable to most of the other values.

From the FT-IR studies, we generate a transmission spectrum from λ = 2.5 μm to 10 μm. Figure 4 shows a comparison of a portion of our analog spectrum with a VIMS transmission spectrum due to aerosol from [2]. The pink shading indicates absorption present at 3.4 μm in the VIMS observation and in our analog but absent in spectra generated from optical constant data from [3].

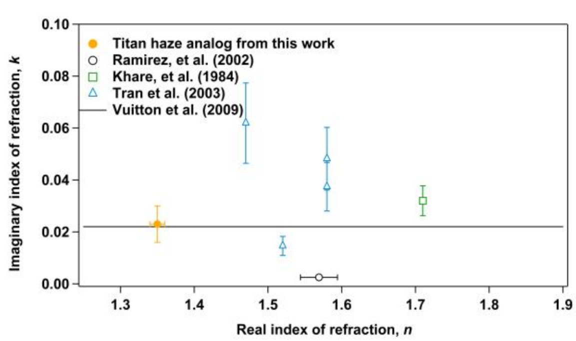

Figure 3: Comparison of refractive indices measured in this study with those from other works. All values from other studies are linearly interpolated to λ = 532 nm.

Discussion: The results for the CRD-AES studies indicate that our UV-generated aerosol generated in a flow system have a smaller real refractive index and a similar imaginary refractive index to Titan aerosol analogs from other studies. Using the refractive indices from this study to calculate extinction of fractal aggregates containing varying numbers of monomer units, the extinction is a factor of 2 to 3 smaller than if values from [3] are used. This has important implications for spacecraft retrievals. The next step in this work is to expand these measurements to other wavelengths.

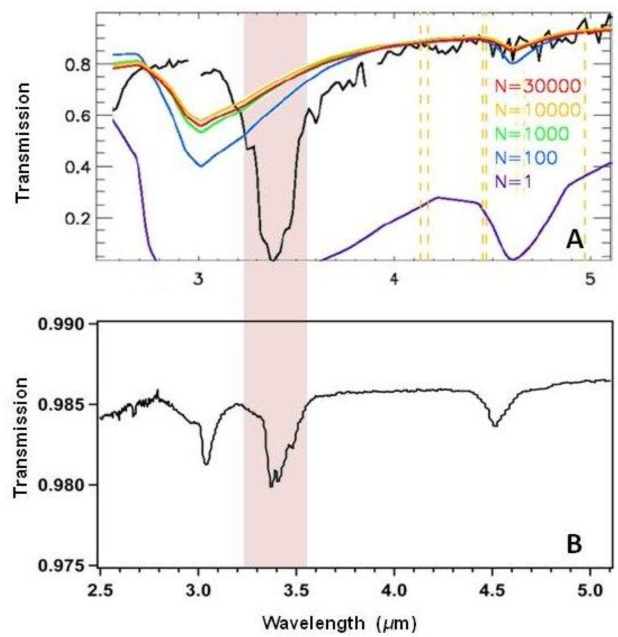

Figure 4: (A) Originally from [2]. Comparison of transmission spectrum observed by Cassini's Visual and Infrared Mapping Spectrometer (VIMS) at 203.16 km (black line) with calculated transmission spectra of fractal aggregates containing various numbers of monomer units N (colored lines). The optical constants of the fractal aggregates are based on values from [3]. This figure has been altered from the original to only show the wavelength range that overlaps with our measurements and to indicate the legend for N. (B) Our measured transmission spectrum from a film of collected Titan analog aerosol. This particular film was generated from a 10% CH_4 in N_2 gas mixture. (B) is also truncated to show the region that overlaps with the VIMS observation.

The FT-IR studies indicate absorption at 3.4 μm in both the VIMS and our spectrum. Absorption at 3.4 μm is thought to be due to aliphatic chains attached to the aerosol [2]. This absorption is not present in spectra generated from optical constant data from [3]. The FT-IR studies provide an interesting comparison to a pressure study performed by [4]. Future work will focus on measuring optical constants of these films.

References: [1] Trainer et al. (2006) *PNAS, 103*, 18035-18042. [2] Bellucci A. et al. (2009) *Icarus*, *201*, 198-216. [3] Khare B. N. et al. (1984) *Icarus*, *60*, 127-37. [4] Imanaka, H. et al. (2004) *Icarus*, *168*, 344-366.